Proceedings World Geothermal Congress 2020+1
Reykjavik, Iceland, April - October 2021

Impact of Scaling on Electrical Submersible Pumps concerning Heat and Power Production of Geothermal Plants and Optimization of Acidification Intervals

Matthäus Irl, Christopher Schifflechner, Christoph Wieland, Hartmut Spliethoff

Technical University of Munich, Institute for Energy Systems, Boltzmannstr. 15, 85748 Garching, Germany

E-mail address of the corresponding author: matthaeus.irl@tum.de

Keywords: Electrical submersible pump, scaling, acidification, condition monitoring of scaling, optimization of operation, economic optimization

ABSTRACT

The number of geothermal plants using deep hydrothermal energy from the South German Molasse Basin has rapidly grown in the last ten years. At the end of 2018, 26 geothermal plants were in operation; five of these are geothermal plants with heat and power production. To forward the thermal brine from the underground, all 26 geothermal plants are using an electric submersible pump, which is a crucial component for reliable and efficient operation. Especially when the brine temperature exceeds 120 °C, which applies to all mentioned geothermal power plants, formation and deposition of scaling in the electrical submersible pump are challenging and cause deterioration of hydraulic performance indicators, e.g., a decrease in mass flow rate of thermal brine, which significantly affects the production of heat and power. A measure to counteract the drop in power caused by scaling is the acidification of the electrical submersible pump, which has proven to extend the lifetime and enhance the performance of this component in geothermal applications.

The impact of scaling on electrical submersible pumps of several deep hydro-geothermal plants in the South German Molasse Basin and the effects of acidification of the electrical submersible pumps are investigated. Long-term operational data of electrical submersible pumps are processed, analyzed and evaluated. Trends of the main operational metrics and key performance indicators of four considered electrical submersible pumps in three geothermal plants are investigated and discussed. Similar trends in the main operational metrics and key performance indicators are identified for the operation of various electrical submersible pumps. As the results show, acidifications of electrical submersible pumps have similar positive effects on their operation and improve their main operational metrics and key performance indicators.

After analyzing the operation of the electrical submersible pumps, a simulation model for a two-stage Organic Rankine Cycle power plant is developed to quantify the losses in electricity production and the related reduction in revenues, caused by the decrease of the thermal brine volume flow rate. Furthermore, scenario analyses of different acidification intervals are carried out to optimize acidification intervals economically and thus achieve a minimal amount of lost revenues associated with a minimal sum of costs for acidifications. As the results show, acidifications of the ESPs influence the operation significantly, and optimizing acidification intervals can considerably increase the profitability of the considered geothermal plants.

1. INTRODUCTION

The South German Molasse Basin (SMB) is currently the most promising and active region for the utilization of hydro-geothermal resources in Germany (Schifflechner et al., 2019). The SMB contains attractive hydrothermal reservoirs that have an average thickness between 400 and 600 m and are located in a depth of between 2 and 5 km (Flechtner and Aubele, 2019). In 2018, 26 projects were operating in the SMB, with a total installed capacity of 296 MW_{th} and 34 MW_{el} (Flechtner and Aubele, 2019). All geothermal plants within the SMB are using electrical submersible pumps (ESP) to lift the brine. The ESPs are a crucial component for the reliable and efficient operation of the geothermal plants. This refers mainly to the high electrical demand of the ESP, which can be more than 20 % of the generated turbine power (Eyerer et al., 2017), and the low reliability and lifetime (Kullick and Hackl, 2017). Since the ESP is installed in several hundred meters depths, condition monitoring is only possible based on the available measurement data, but the measurement technologies of the pumps often fail completely or display implausible values. Additionally, repairing or replacing the ESP comes along with long downtime periods as well as high costs for the operator. These issues are also related to the formation and allocation of scaling, which is not only a major problem for the ESPs, but can also affect the operation of the pipes, filters and heat exchangers significantly (Köhl and Baumann, 2018). Scaling describes the formation of solids within a solution, which is caused by an oversaturation of a certain salt (Frick et al., 2011). The saturation depends on the fluid's characteristics such as pH-value, temperature, and pressure as well as the concentrations of different dissolved solids and gases. In the SMB, the majority of the encountered scalings are carbonates, which are formed due to a disruption of the lime-carbonic-acid equilibrium, shown in Equation 1, during production triggered by the degassing of CO_2 (Köhl and Baumann, 2018). The lime-carbonic-acid

$$H_2CO_3{}^* + CaCO_3(s) \rightleftharpoons Ca^{2+} + 2\,HCO_3{}^- \tag{1}$$

equilibrium is mainly influenced by the concentration of carbon acid, which in turn is reliant on the concentration of solute carbon dioxide, according to Equation 2. Depending on the pH-value of the water solution, carbonic acid is dissolved in $HCO_3{}^-$ or $CO_3{}^{2-}$. The basics of the lime-carbonic-acid equilibrium are described in Wisotzky et al. (2018) in detail.

$$H_2O + CO_2 \rightleftharpoons H_2CO_3 \tag{2}$$

The concentrations of ions as well as of solute gas influencing the lime-carbonic-acid equilibrium are depicted in Table 1 for the three investigated geothermal plants relative to each other. The in situ measured pH-values are between 6.3 and 6.4 for all investigated geothermal plants. The water samples were taken at the surface under pressure in steel cylinders and analyzed in the laboratory.

Table 1: Concentrations of ions as well as of solute gas influencing the lime-carbonic-acid equilibrium of the three investigated geothermal plants relative to each other

	Geothermal Plant A	Geothermal Plant B	Geothermal Plant C
Concentration of ions in %			
Calcium (Ca^{2+})	100,0	70,6	93,5
Hydrogen carbonate (HCO_3^-)	100,0	92,0	97,6
Concentration of solute gas in %			
Carbon dioxide (CO_2)	77,6	78,7	100,0

The thermal brine temperatures measured at the wellhead differ by a few degrees Celsius. Entirely slight disparities in the concentrations and pH-values of the three investigated geothermal plants can be ascertained, which means that formation and allocation of scaling in the investigated ESPs are mainly dependent on the design and operation of the ESPs and not of the thermal brine composition. Any data or measurements to specify the physical or chemical conditions in the thermal reservoirs were not available.

To remove the precipitated calcium carbonate in the ESP eight-percent hydrochloric acid is used. For this purpose, the ESP is shut down and a pipe is installed in the rising pipe of the ESP. Hydrochloric acid is injected a few meters above the ESP and the pipe is removed. After an application time of about six hours the ESP is started and the mixture of brine, hydrochloric acid, and formed calcium chloride is discharged from the thermal water system and disposed of in a controlled manner.

While the effect of scaling on the performance of heat exchangers is investigated by several studies (cf. (Milanovic et al., 2006; Zarrouk et al., 2014)), no detailed studies about the effect on ESPs exist. Ravier et al. (2015) present the issues with line shaft pumps (LSP) caused by the aggressive geothermal water condition of the geothermal plant in Soultz. Kullick and Hackl (2017) developed a detailed dynamic model of a geothermal ESP, which might also be used for condition monitoring in the future. While both studies discuss several general aspects with respect to improved condition monitoring and maintenance of ESPs, they are not considering long-term operational data for the evaluation. Thus, no detailed conclusions about the expected behavior of newly installed ESPs can be drawn. However, profound knowledge about the expected degradation processes of real ESPs with increasing lifetime is of high interest for plant operators and researchers to improve the performance of geothermal plants. Therefore, this study investigates the degradation processes occurring for four ESPs installed at three real geothermal plants in the SMB. For this purpose, long-term operational data are analyzed. A statement about the expected degradation process over the ESP's lifetime is postulated based on the behavior of suitable key performance indicators. In the next step, a simulation model for a two-stage Organic Rankine Cycle power plant is developed to quantify the losses in electricity production caused by the decrease of the thermal brine mass flow rate. Several scenarios with varied acidification intervals are analyzed at different lifetime points of the electric submersible pumps. The possibility of significantly higher financial revenues due to improved acidification intervals are discussed.

2. METHODOLOGY

For all investigated geothermal plants, long-term operational data in a total of more than eight years of operation are present. In addition, information about the installed pump types, the installed pump depths as well as dates of pump changes and acidifications are known. Since this work focuses on the long-term behavior of the ESPs and not on the short-term behavior during start-up and shutdown processes and due to a better visualization in graphs, filter criteria ensure that only operational data during steady-state operation, respectively during operation with low gradients of the main process variables, are considered. Therefore, predominantly thresholds for the minimum frequency of AC power after the converters of ESPs, the minimum thermal brine volume flow rate and the minimum turbine power are applied. Since the quality of the long-term operation results essentially depends on the quality of the input data for the analyses and calculations, great effort was put into the validation of the mass flow rates and the generated turbine power. Mass and energy balances of various measuring instruments, heat exchangers and turbines were used for the validation. In addition, uncertainties of the measured values were calculated with consideration of the entire measuring chains.

The filtered data are evaluated with respect to changes in the measured values (thermal brine mass flow rate, pressures, etc.) as well as performance indicators. Two potential performance indicators are the mass-specific pump power MSP and the pump system efficiency $\eta_{sys,pump}$. The MSP describes the ratio between the required electrical pump power and the pumped mass flow (DiPippo and Moya, 2013). Therefore, the MSP represents the required amount of electrical power for lifting one kg of thermal water per second.

$$MSP = \frac{P_{el,pump}}{\dot{m}_{brine}} \tag{3}$$

For plant operators, a low as possible MSP is favorable, since this means that only a small amount of electrical power is required to lift one kg of thermal water per second. However, the achievable MSP of a geothermal plant is strongly influenced by the individual local geological and hydraulic conditions and is therefore only limited suited for benchmarking between different geothermal plants.

When using it for condition monitoring at one particular plant, an increase of the MSP could be the first indication of an occurring deterioration, but since this performance indicator does not consider the pressure levels around the pump, potential performance degradations might be not detected. The pump system efficiency $\eta_{sys,pump}$ overcomes this limitation, since this performance indicator considers the thermal brine volume flow rate, the electrical power demand of the pump and the overall delivery head $DH_{overall}$ (Beebe, 2004).

$$\eta_{sys,pump} = \frac{\rho_{brine} \cdot g \cdot \dot{V}_{brine} \cdot DH_{overall}}{P_{el,pump}} \tag{4}$$

The overall delivery $DH_{overall}$ head consists of three different components:

$$DH_{overall} = DH_{geo} + DH_{fric} + DH_{wh} \tag{5}$$

The geodetic delivery head DH_{geo} represents the height difference between the water level outside the rising pipe and the wellhead (cf. Fig. 1). DH_{fric} considers the necessary head to overcome the friction losses within the rising pipe. Since the wellhead pressure is higher than the ambient pressure, the pressure head at the wellhead DH_{wh} must be taken into account as well. Next to these two

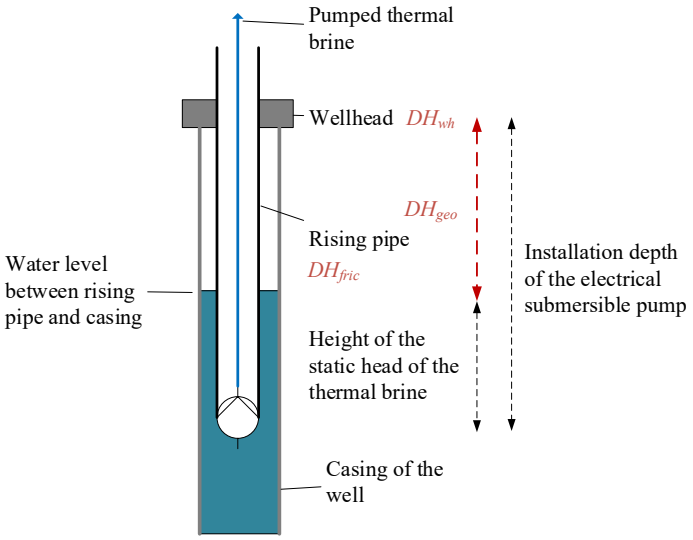

Figure 2: Schematic drawing of the thermal water pump system with the delivery heights to be considered

performance indicators, the observation of the operating point in comparison to the expected performance curves for the corresponding frequency within the pump diagram might also provide useful insights about potential condition changes of the pump (Beebe, 2004; Ravier et al., 2015).

For one of the evaluated geothermal plants, the possibility of improved acidification intervals is investigated. For this purpose, the additional achievable revenues I_{add} due to the higher flow rate caused by the acidification are compared to the costs of the acidification C_{acid} as well as the occurring lost revenues due to the necessary downtime period of the plant during the acidification C_{down}. The variable n represents the number of acidifications.

$$Financial\ impact = I_{add} + C_{acid} \cdot n + C_{down} \cdot n \tag{6}$$

3. ANALYSIS OF THE LONG-TERM OPERATIONAL DATA OF FOUR ELECTRICAL SUBMERSIBLE PUMPS

In this section, the trend as a function of the operating days of the main operational measured metrics as well as in section 2 previously introduced key performance indicators of the four investigated ESPs are presented, evaluated and discussed at the end of this section.

3.1 Trend of the thermal brine mass flow rate, AC power frequency, and electrical power consumption

Figure 1 displays the trend as a function of the operating days of the normalized thermal brine mass flow rate, the preset AC power frequency generated by the frequency converter of the AC power source inducing the magnetic field in the stator of the ESP motor, and the electrical power consumption of the ESPs. Furthermore, times of acidification of the four investigated ESPs are marked in the diagrams. Thermal brine mass flow rates and electrical power consumptions are normalized to their highest values occurring in the investigated period. In terms of better comparability, a constant value was used to normalize the AC power frequency. As shown in Fig. 1, the operation of the four investigated ESPs of the three considered geothermal plants lasted from 343 up to 615 days. One to three acidifications of the ESPs were carried out in their lifetimes. The first acidification occurred in most of the cases after approximately seven months. The thermal brine mass flow rate increased after the first acidification in all geothermal plants. Although the AC power frequency of Pump 1 in Geothermal Plant A was lower after the acidification than before, the thermal brine mass flow rate increased slightly. The first acidification of Pump 1 in Geothermal Plant C leads to the highest increase of +18.9 % of the thermal brine mass flow rate. The second acidification also showed positive effects on the thermal brine mass flow rate in all cases. The third acidification of Pump 1 in Geothermal Plant C resulted only in a low increase of the thermal brine mass flow rate. The peak of the

thermal brine mass flow rate immediately after the third acidification is not plausible and is most likely caused due to malfunction of the volume flow rate sensor.

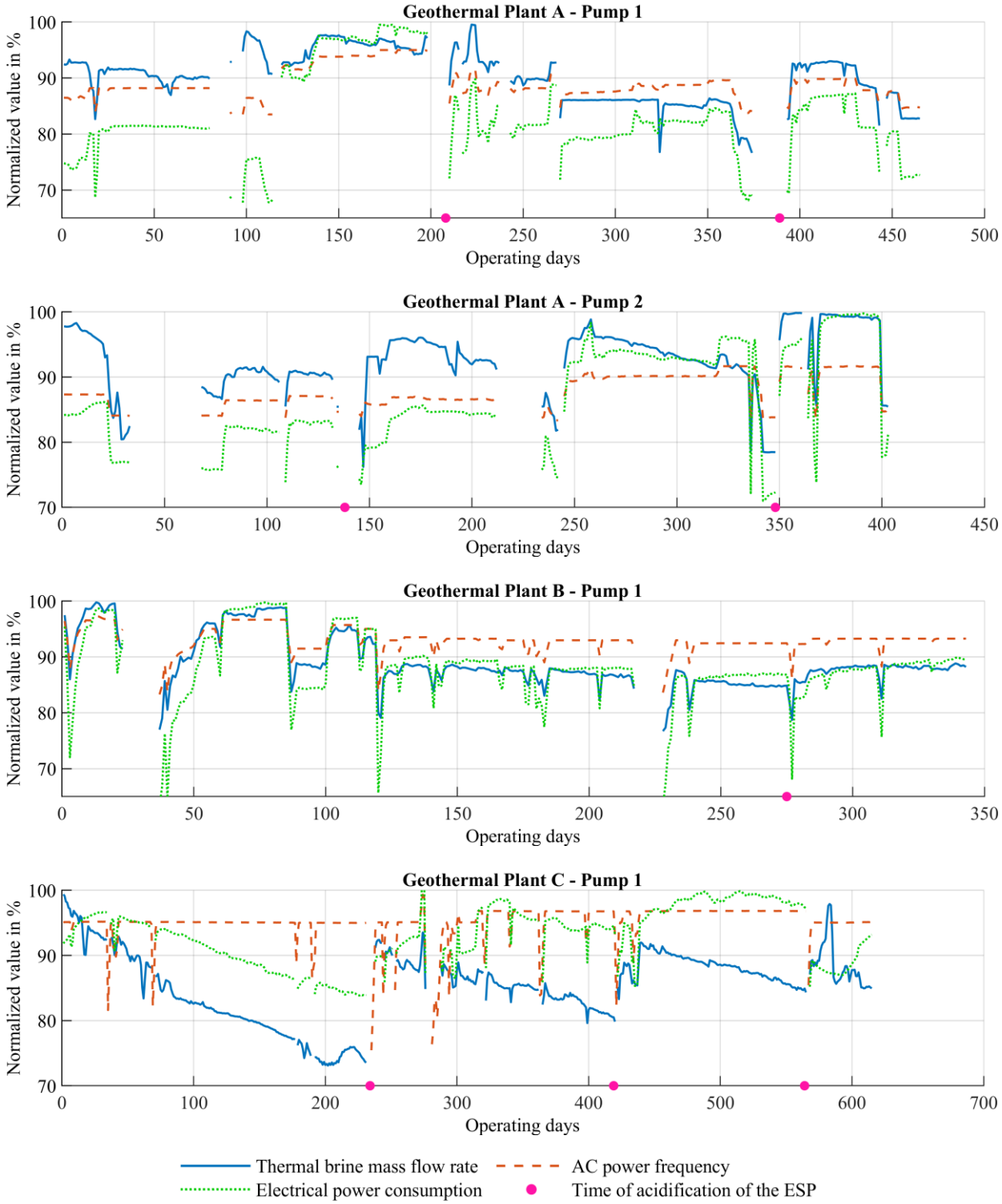

Figure 3: Daily averaged normalized thermal brine mass flow rate, AC power frequency, electrical power consumption and time of acidification of the investigated ESPs

The electrical power consumption of the ESPs correlates strongly with the thermal brine mass flow rate as can be seen in the diagrams of all geothermal plants. Thus, higher thermal brine mass flow rates lead to higher electrical power consumption after acidifications of the ESPs. The trend of the electrical power consumption of Pump 1 in Geothermal Plant C after the second and third acidification is remarkable due to the fact that it rose with decreasing thermal brine mass flow rate.

3.2 Trend of the delivery heads

Next to thermal brine mass flow rate, electrical power consumption, and AC power frequency, the overall delivery head is crucial to assess the performance of an ESP. Therefore, Fig. 3 visualizes the trend of the overall delivery head as well as its single components

(cf. Equation 5) for all investigated ESPs. Although in Fig. 3 all components are nominalized to their respective maximum, it can be clearly stated that the geodetic head mainly influences the overall delivery head, while the other two components have only a small

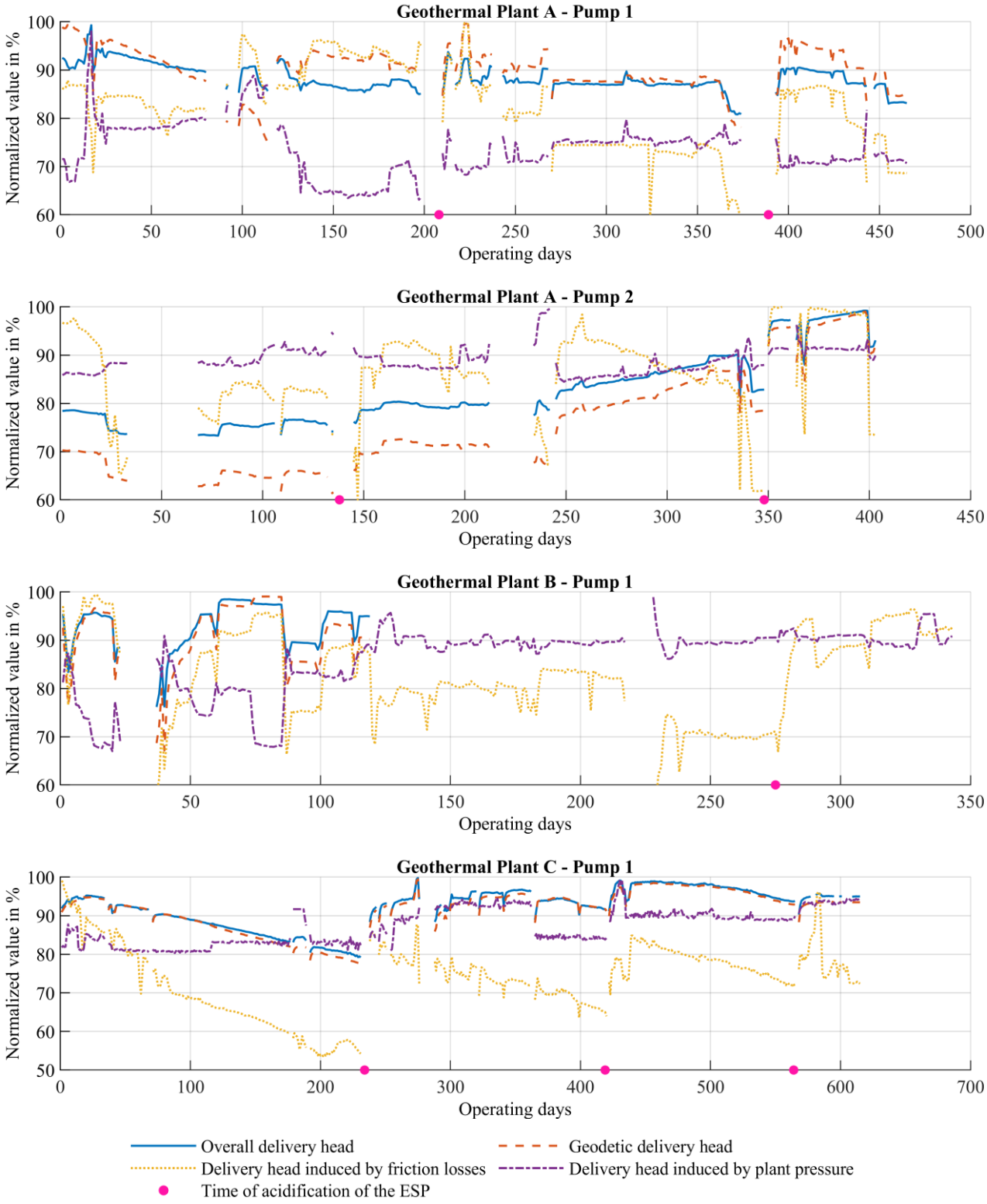

Figure 4: Daily averaged normalized delivery heads to be considered of the investigated ESPs

share. The overall delivery head of Pump 1 in the Geothermal Plant A and Geothermal Plant C reveals the same general behavior. For both ESPs, the overall delivery head decreased with time. Of course, the figure also shows an inevitable fluctuation of the overall delivery head, but this behavior appears mainly caused by changes in the AC power frequency (cf. Fig. 2). The overall delivery head increased for both ESPs after the acidifications. Pump 2 in Geothermal Plant A shows an opposing behavior. Here, the overall delivery head increased significantly over time. Even in periods with constant frequency and decreasing mass flow (cf. operating days 250 – 325 in Fig, 2), the geodetic delivery head increased. This behavior cannot be explained entirely. However, it is estimated that it must be caused by changes occurring in the thermal water reservoir. For Pump 1 in Geothermal Plant B, no statement about the long-term

behavior is possible, since the measurement of the pressure at the pump inlet failed after around 120 operating days. Thus, no calculations of the geodetic delivery head were possible after this time.

Combining the observations from Fig. 2 and 3 reveals that the behavior of the delivery head caused by friction losses is directly linked to the trend of the pumped thermal brine mass flow rate. Since the density of the thermal water was approximately mainly constant, the mass flow rate dominates the velocity within the rising pipe and therefore also the induced friction losses. The delivery head due to the pressure level was also varying over time. This is mainly caused by minor changes of the operation strategy of the above-surface thermal water system.

3.3 Trend of the pump system efficiencies and the mass-specific pump powers

To evaluate the performance of the ESPs, the systematic ESP system efficiency as well as the mass-specific pump power are analyzed (cf. Equation 3 and 4), which normalized trends are depicted in Fig. 4. For Pump 1 installed in Geothermal Plant A, the ESP system efficiency was decreasing over time. The short "jump" of this key performance indicator around day 100 is expected to be caused by a temporary issue with the measurement technology of the thermal brine volume flow rate. Within the first 200 days, the normalized pump efficiency decreased by about 25 %. After the acidifications of Pump 1 in Geothermal Plant A, the ESP system efficiency increased significantly. The MSP was growing with time, while the acidifications cause a significant reduction. Pump 2 at the same plant shows a bit different behavior. Here, the ESP system efficiency decreased slightly with increasing operation time (e.g., during the period 0 – 130 days and 150 – 340 days), but the highest ESP system efficiency is reached after the second acidification. This might lead to the conclusion that the ESP would have been working more efficient after 350 days in operation since at its initial operation, but Section 3.2 showed that the geodetic delivery head and thus the overall delivery head of this pump increased significantly during this time, which might have been significantly effected the operating point in the speed-torque diagram of the asynchronous motor of the ESP. For Pump 1 in Geothermal Plant B, the ESP system efficiency decreased slightly before the pressure measurement ended. The ESP in Geothermal Plant C reveals a significant decrease in the ESP's system efficiency during operation. After operation began, the ESP system efficiency decreased from 100 % to 70 % in around 230 days. The first acidification helped to increase the ESP system efficiency again close to 95 % before it started to decrease again. The same behavior also appeared after the next two acidifications.

The MSP increased over time, while the acidifications caused a significant decrease in this key performance indicator. However, the comparison between both key performance indicators reveals that during periods with constant MSPs (e.g., during the days 100 and 180), the ESP system efficiency is able to detect ongoing degradation processes.

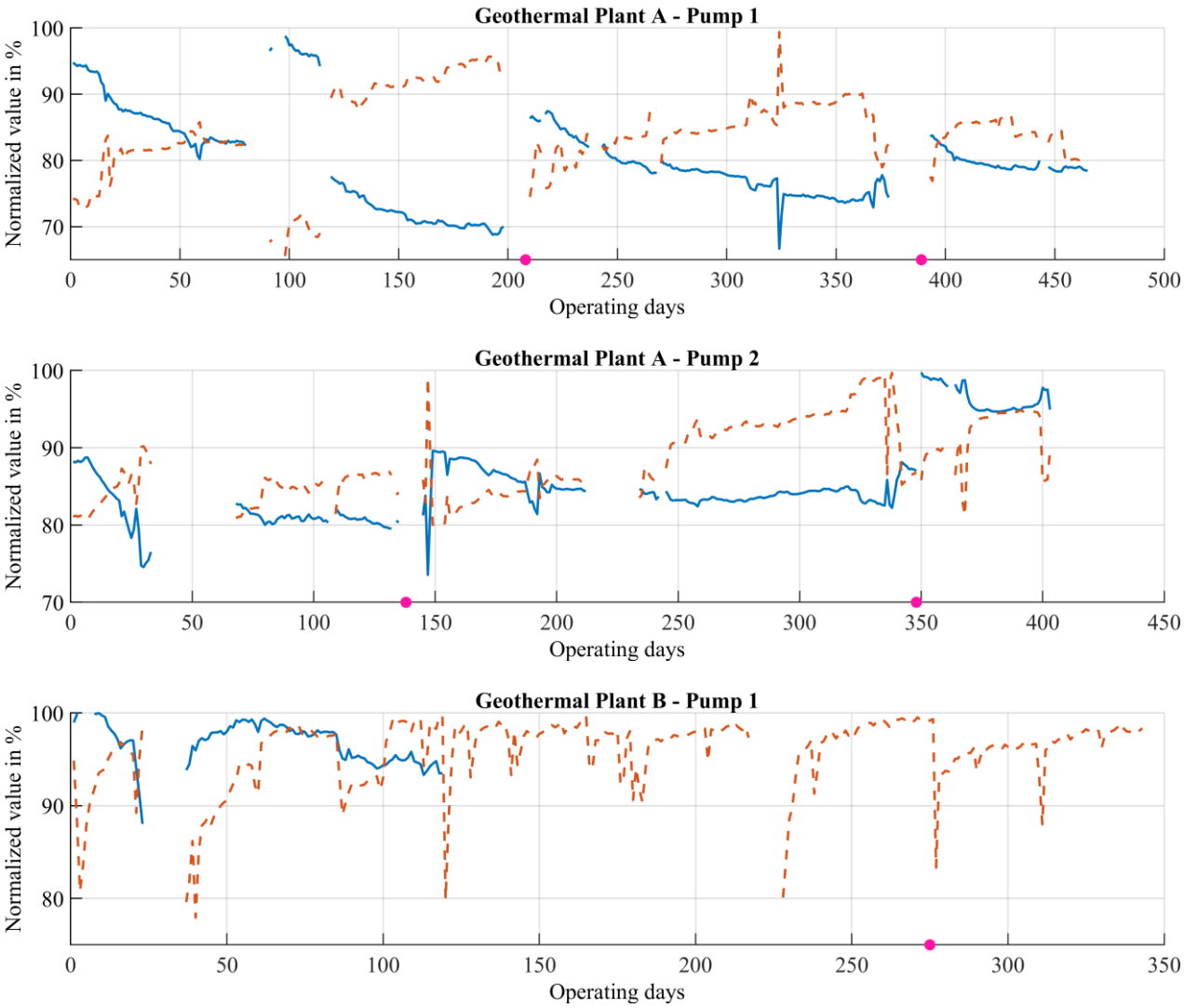

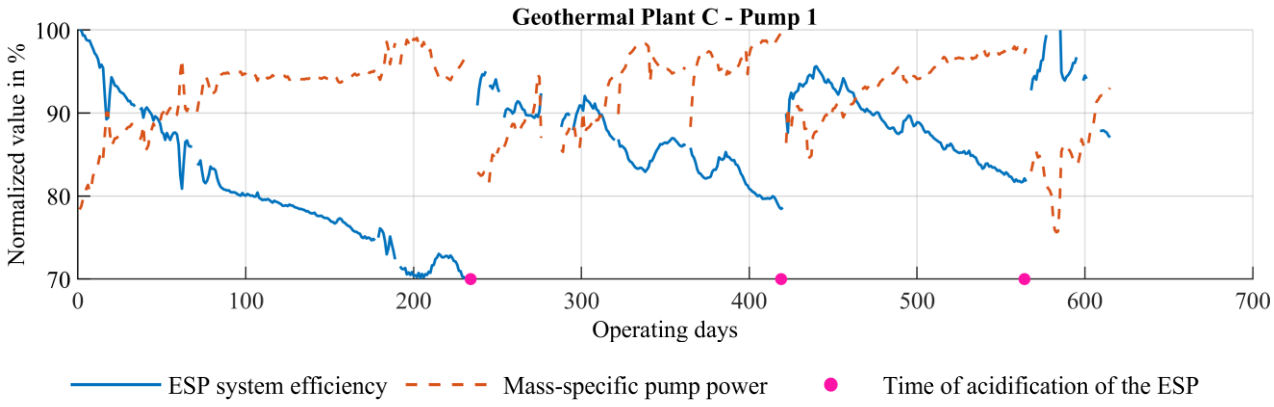

Figure 5: Daily averaged normalized Pump system efficiency and mass-specific pump power of the investigated ESPs

3.4 Analysis and assessment of the acidifications of the ESPs

In Fig. 5 are the differences in the normalized values of the in the previous section displayed main operational metrics and key performance indicators between after and before the first acidifications of the ESPs depicted. For the determination of the differences, operating points immediately before and after acidification were not necessarily taken into account, but stationary operating points were decisive. Although the setpoints of the AC power frequency were lower in two of the four investigated geothermal plants after the first acidification, the thermal brine mass flow rate increases in all geothermal plants after the first acidification. Fig. 5 reveals that the increases in thermal brine mass flow rates are different. If the AC power frequency of Pump 1 in Geothermal Plant A had been the same after the first acidification, the thermal brine mass flow rate would have been higher, since small changes in the AC power frequency have a significant impact on the thermal brine mass flow rate. Nevertheless, an increase of 5 % of the thermal brine mass flow rate increases the turbine output power of the power plant significantly. The first acidification of Pump 1 after almost eight months of operation in Geothermal Plant C shows the highest increase of 18.9 %, which is striking. Furthermore, the overall delivery heads of all investigated ESPs increased, even though it is obvious for Pump 1 in Geothermal Plant A as the frequency was lower. The values of the differences in the electrical power consumption alone do not allow conclusions to be drawn, but must be interpreted in conjunction with other values like the thermal brine mass flow rate and the mechanical power of an ESP. The mass-specific pump power decreases from -3.4 % to -14.2 % after the acidifications of the ESPs. The relative ESP system efficiencies show the highest increase of all considered main metrics and key performance indicators from 9 % up to 24.7 %, which means fewer costs for the electrical power consumption accompanied by higher thermal brine mass flow rates. Therefore it can be concluded that the first acidification is expedient and has a major impact on the operation of the investigated ESPs.

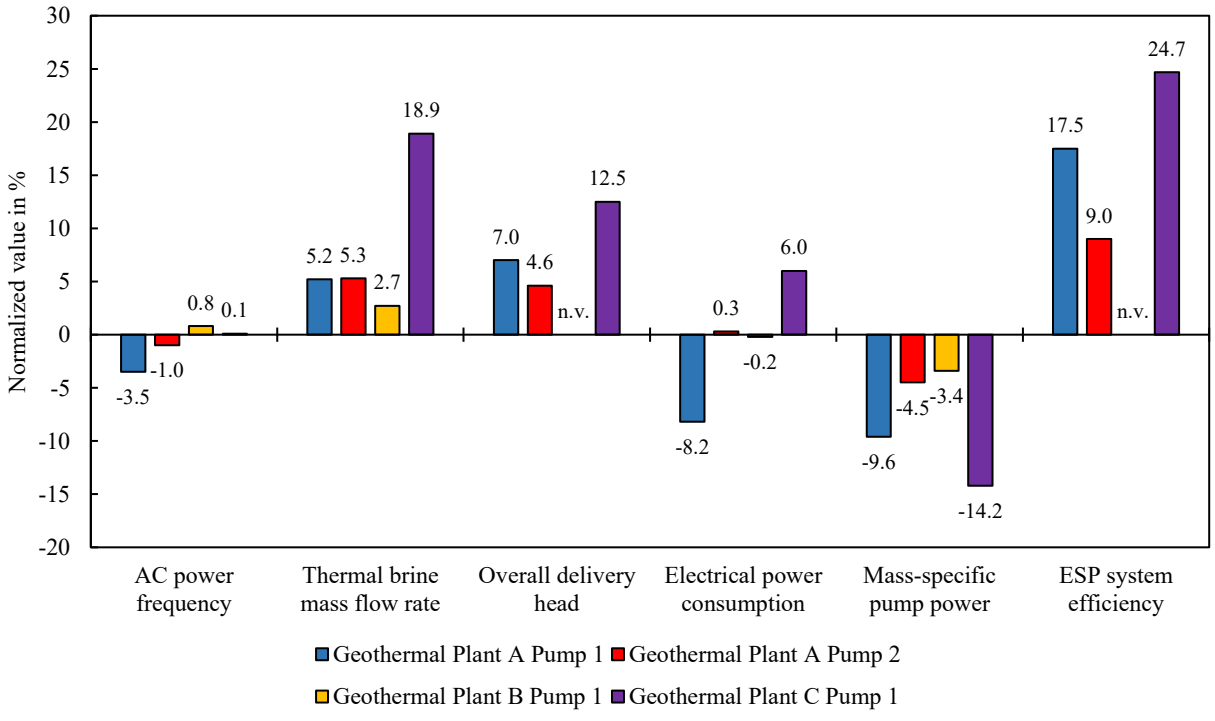

Figure 6: Differences of the normalized values of the main operational metrics and key indicators after and before the first acidification of the ESPs

Fig. 6 shows the differences in the normalized values of the main operational metrics and key indicators between after and before the second acidifications of the ESPs. The AC power frequencies of the ESPs were equal after the second acidifications. Against this

backdrop, the main metrics and key indicators are meaningful comparable. The thermal brine mass flows exhibit the same amount of increase up to 8.6 %. The delivery heads have also significantly increased, and the differences are in two cases similar, whereas the electrical power consumptions of the ESPs have hardly changed. The average value of the decreases of the mass-specific pump powers caused by the second acidifications was according to amount comparatively higher than for the first acidifications. The relative ESP system efficiencies also increased considerably for all three investigated second acidifications. The differences of the normalized values of the main metrics and key indicators show the same trend for the third acidification of Pump 1 in Geothermal Plant C as for the previous acidifications.

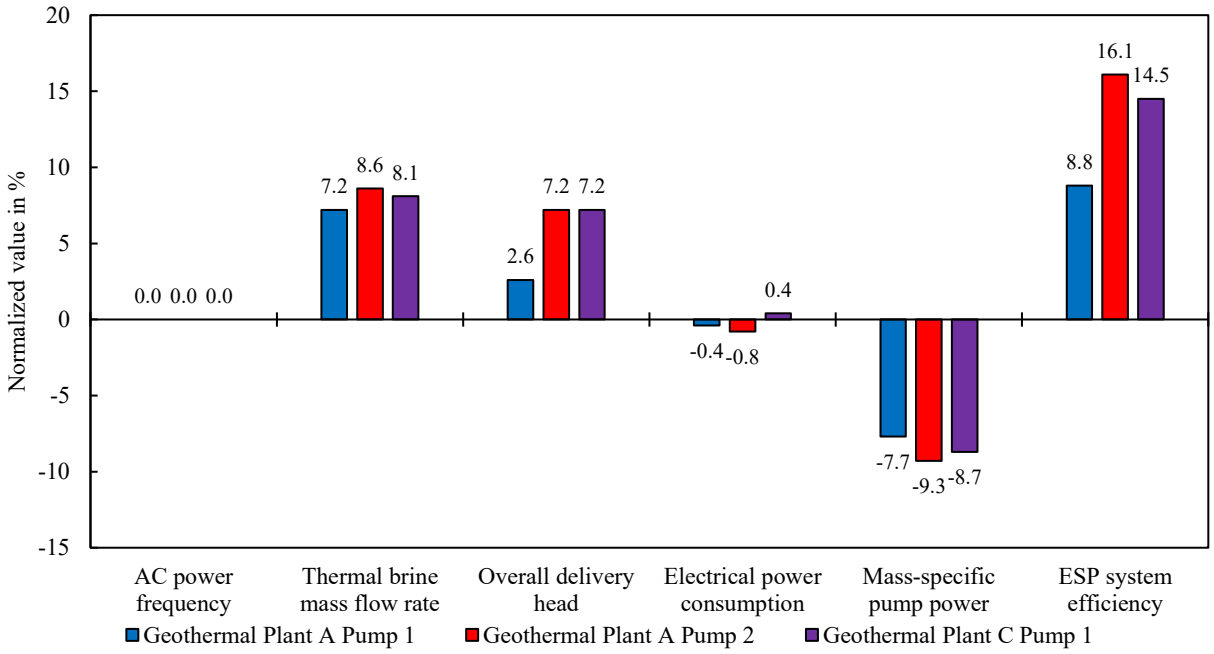

Figure 7: Differences of the normalized values of the main operational metrics and key indicators after and before the second acidification of the ESPs

Figure 7 displays the between two operating time points averaged gradients of the normalized ESP system pump efficiencies dependent on the operating days of the pumps. The averaged gradient of the normalized ESP system efficiency of Pump 1 in Geothermal Plant A exhibits the same time behavior as Pump 1 in Geothermal plant C. After the commissioning of both ESPs until the first acidification, the normalized ESPs system pump efficiencies decreased by about 0.13 % per operating day. The gradient of the normalized pump efficiencies of Pump 1 in Geothermal Plant A increased according to amount over its whole lifecycle while the gradient of Pump 1 in Geothermal Plant C was constant after the second acidification. The gradients of Pump 2 in Geothermal Plant A were much lower compared to the gradients of the other pumps for the major part of its lifecycle and assumed roughly the same values in the range of 350 to 400 operating days.

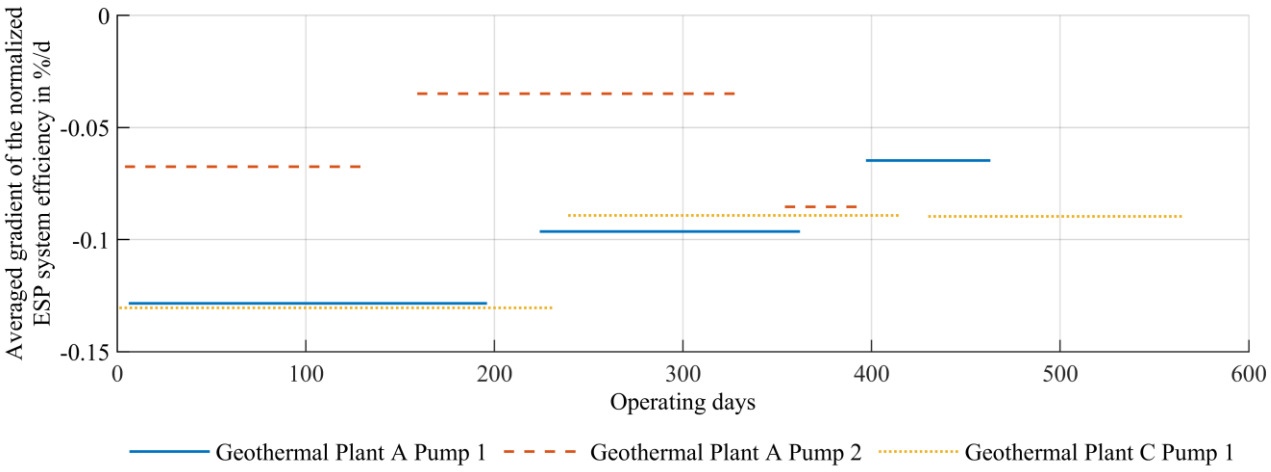

Figure 8: Between two operating time points averaged gradients of the normalized ESP system pump efficiencies

All values of the normalized main metrics and key performance indicators at previously mentioned time points in the lifecycle of the investigated ESPs can be found in Table 2.

Table 2: Values of the normalized main metrics and key performance indicators at specific time points in the lifecycle of the investigated ESPs

		Com-mis-sioning	Before the first acidification	Differ-ence	Gradient in %/d	After the first acidification	Differ-ence	Before the second acidification	Differ-ence	Gradien t in %/d	After the second acidification	Differ-ence	Before the third acidification	Differ-ence	Gradien t in %/d	After the third acidification	Differ-ence	Taking out of operation	Differ-ence	Gradien t in %/d	Overall difference
GP A P 1	Operating days	6	196	190		224	-	362	138		397	-	-	-	-	-	-	465	68	-	459
	AC power frequency	86,1	95,0	8,9	0,047	91,5	-3,5	89,6	-1,9	-0,014	89,6	0,0	-	-	-	-	-	84,7	-4,9	-0,072	-1,4
	Thermal brine mass flow rate	92,8	94,3	1,5	0,008	99,5	5,2	85,4	-14,1	-0,102	92,6	7,2	-	-	-	-	-	82,8	-9,8	-0,144	-10,0
	Overall delivery head	90,4	85,3	-5,1	-0,027	92,3	7,0	87,6	-4,7	-0,034	90,2	2,6	-	-	-	-	-	83,3	-6,9	-0,101	-7,1
	Electrical power consumption	73,8	98,0	24,2	0,127	89,8	-8,2	83,9	-5,9	-0,043	83,5	-0,4	-	-	-	-	-	72,6	-10,9	-0,160	-1,2
	Mass specific pump power	72,9	92,4	19,5	0,103	82,8	-9,6	90,1	7,3	0,053	82,4	-7,7	-	-	-	-	-	80,5	-1,9	-0,028	7,6
	ESP system efficiency	94,2	69,8	-24,4	-0,128	87,3	17,5	74,0	-13,3	-0,096	82,8	8,8	-	-	-	-	-	78,4	-4,4	-0,065	-15,8
GP A P 2	Operating days	4	130	126	-	160	-	332	172	-	354	-						395	41	-	391
	AC power frequency	87,3	87,0	-0,3	-0,002	86,0	-1,0	91,7	5,7	0,033	91,7	0,0	-	-	-	-	-	91,5	-0,2	-0,005	4,2
	Thermal brine mass flow rate	98,0	90,4	-7,6	-0,060	95,7	5,3	91,0	-4,7	-0,027	99,6	8,6	-	-	-	-	-	98,7	-0,9	-0,022	0,7
	Overall delivery head	78,5	75,4	-3,1	-0,025	80,0	4,6	89,8	9,8	0,057	97,0	7,2	-	-	-	-	-	99,0	2,0	0,049	20,5
	Electrical power consumption	84,3	83,2	-1,1	-0,009	83,5	0,3	95,6	12,1	0,070	94,8	-0,8	-	-	-	-	-	99,4	4,6	0,112	15,1
	Mass specific pump power	81,2	86,8	5,6	0,044	82,3	-4,5	98,9	16,6	0,097	89,6	-9,3	-	-	-	-	-	94,8	5,2	0,127	13,6
	ESP system efficiency	88,2	79,7	-8,5	-0,067	88,7	9,0	82,7	-6,0	-0,035	98,8	16,1	-	-	-	-	-	95,3	-3,5	-0,085	7,1
GP B P 1	Operating days	19	274	255	-	286	-	-	-	-	-	-	-	-	-	-	-	343	57	-	324
	AC power frequency	96,8	92,5	-4,3	-0,017	93,3	0,8	-	-	-	-	-	-	-	-	-	-	93,3	0,0	0,000	-3,5
	Thermal brine mass flow rate	99,2	84,8	-14,4	-0,056	87,5	2,7	-	-	-	-	-	-	-	-	-	-	88,5	1,0	0,018	-10,7
	Overall delivery head	95,0	n. v.	n. v.	n. v.	n. v.	n. v.	-	-	-	-	-	-	-	-	-	-	n. v.	n. v.	n. v.	n. v.
	Electrical power consumption	98,4	86,7	-11,7	-0,046	86,5	-0,2	-	-	-	-	-	-	-	-	-	-	89,5	3,0	0,053	-8,9
	Mass specific pump power	96,2	99,1	2,9	0,011	95,7	-3,4	-	-	-	-	-	-	-	-	-	-	98,4	2,7	0,047	2,2
	ESP system efficiency	96,9	n. v.	n. v.	n. v.	n. v.	n. v.	-	-	-	-	-	-	-	-	-	-	n. v.	n. v.	n. v.	n. v.
GP C P 1	Operating days	1	231	230	-	241	-	417	176	-	430	-	565	135	-	572	-	615	43	-	614
	AC power frequency	95,1	95,0	-0,1	0,000	95,1	0,1	96,8	1,7	0,010	96,8	0,0	96,8	0,0	0,000	95,1	-1,7	95,1	-1,7	-0,040	0,0
	Thermal brine mass flow rate	99,4	73,5	-25,9	-0,113	92,4	18,9	80,7	-11,7	-0,066	88,8	8,1	84,3	-4,5	-0,033	88,7	4,4	85,0	-0,1	-0,002	-14,4
	Overall delivery head	91,8	79,2	-12,6	-0,055	91,7	12,5	91,9	0,2	0,001	99,1	7,2	93,8	-5,3	-0,039	94,5	0,7	95,0	-4,6	-0,107	3,2
	Electrical power consumption	91,9	83,9	-8,0	-0,035	89,9	6,0	94,2	4,3	0,024	94,6	0,4	97,3	2,7	0,020	88,8	-8,5	93,2	-5,8	-0,135	1,3
	Mass specific pump power	78,4	96,7	18,3	0,080	82,5	-14,2	99,0	16,5	0,094	90,3	-8,7	97,8	7,5	0,056	84,6	-13,2	93,0	-5,7	-0,133	14,6
	ESP system efficiency	100,0	70,0	-30,0	-0,130	94,7	24,7	79,0	-15,7	-0,089	93,5	14,5	81,4	-12,1	-0,090	95,2	13,8	87,1	1,7	0,040	-12,9

4. OPTIMIZATION OF ACIDIFICATION PERIODS OF ELECTRICAL SUBMERSIBLE PUMPS

In this section, the amount of electrical energy losses due to the deterioration of the thermal brine mass flow rate caused by scaling and its financial impact of geothermal power plants is investigated. After the determination of the amount of losses of produced electrical energy with a simulation model of a two-staged ORC power plant, scenario analysis of different acidification intervals is carried out to optimize acidification intervals economically. For the investigated ESP 1 in Geothermal Plant C, two different periods from commissioning to the first acidification and from the first to the second acidification are evaluated, since the previous analysis revealed that the gradient of the ESP system efficiency degradation is higher for the first 200 days than for later operating times (cf. Figure 7). Thus, different optimized acidification periods might occur depending on the lifetime of the ESP. Surplus profits dependent on the costs for one acidification of the ESP 1 in Geothermal Plant C are calculated as the main result for the investigated shorter acidification intervals in the two considered periods.

4.1 Determination of the amount of electrical energy losses due to the deterioration of the thermal brine volume flow rate caused by scaling investigating different acidification intervals of the ESP 1 in Geothermal Plant C

Figure 8 visualizes the trend of the volume flow rate degradation within both considered periods. Within the first period between the commissioning and the first acidification, the normalized thermal brine volume flow rate decreased from 100 % to 73 %. Based on the experience of the previous analysis, it is assumed that after the first acidification only 96 % of the initially achievable flow rate can be obtained, since some of the occurring degradation processes during the first months appear to be permanently. Within the second considered period, the normalized volume flow rate decreases from 100 % (which represents 96 % of the volume flow rate after the installation of the new pump) to 90 %. The need for the fitting function is caused by the necessity of a continual function for the later evaluated impact of the flow rate increases due to additional acidifications. Furthermore, temporary reductions of the flow rate or plant shutdowns due to non-ESP related issues (e.g., caused by problems with the electrical grid) should be not considered in the following evaluation, since it aims solely at an assessment of the optimal acidification intervals.

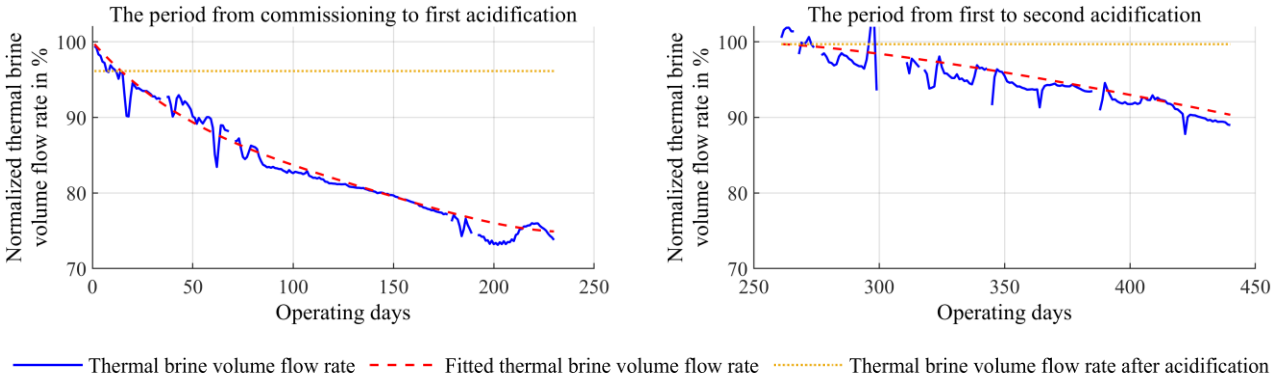

Figure 9: Trend of the thermal brine volume flow rate with increasing operating days and the defined fitting functions representing the thermal brine volume flow rate reduction for the two considered periods of the ESP 1 in Geothermal Plant C

The described reductions of the volume flow rate cause consequently financial losses for the plant operator. To be able to assess these losses, a detailed simulation model of the considered two-staged ORC power plant with a rated power of roughly 5 MW is developed

and validated with real operational data of the ORC power plant. The simulation model is then used to compute both the possible electrical power for the theoretically maximum possible thermal brine volume flow rate and for the actual thermal brine volume flow rate (both for the actual average daily ambient temperature). As Fig. 9 shows, the simulation model works properly since for most of the time, the measured data and the predicted plant power for the fitted thermal brine volume flow rate match satisfactory. Only for days with a thermal brine volume flow rate significantly lower than the fitting model or days with a very low ambient temperature (e.g., around the operating day 125), a slight deviation occurs, which leads to an underestimation of the power losses due to reduced thermal brine volume flow rate caused by scaling. Hence, the losses of the amount of produced electrical energy associated with the financial losses are not overestimated. Furthermore, downtimes of the ORC power plant are excluded for the calculation of the amount of losses of produced electrical energy in the following scenario analysis investigating different acidification intervals.

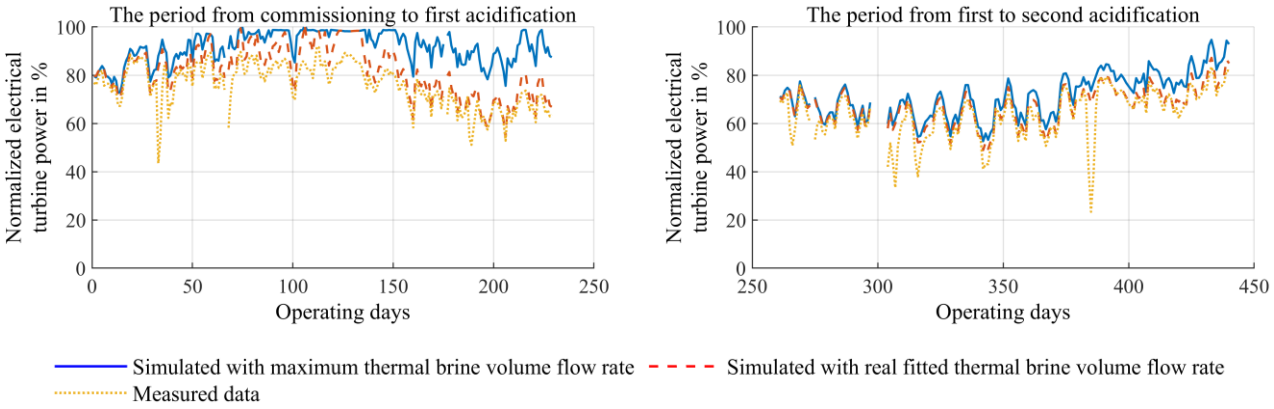

Figure 10: Comparison of the measured electrical power and the simulated electrical power of the two-staged ORC power plant of Geothermal Plant C for the maximal thermal brine flow rate and the real fitted flow rate in the two considered periods

In the next step, the impact of possible shorter acidification intervals is investigated with scenario analysis. For this purpose, hypothetical scenarios with one and two additional acidifications within both considered periods are investigated. It is assumed that after each additional acidification, the maximal obtainable flow rate (cf. Fig. 8) is achieved. Fig. 10 presents the resulting expected normalized thermal brine volume flow rates for the different scenarios.

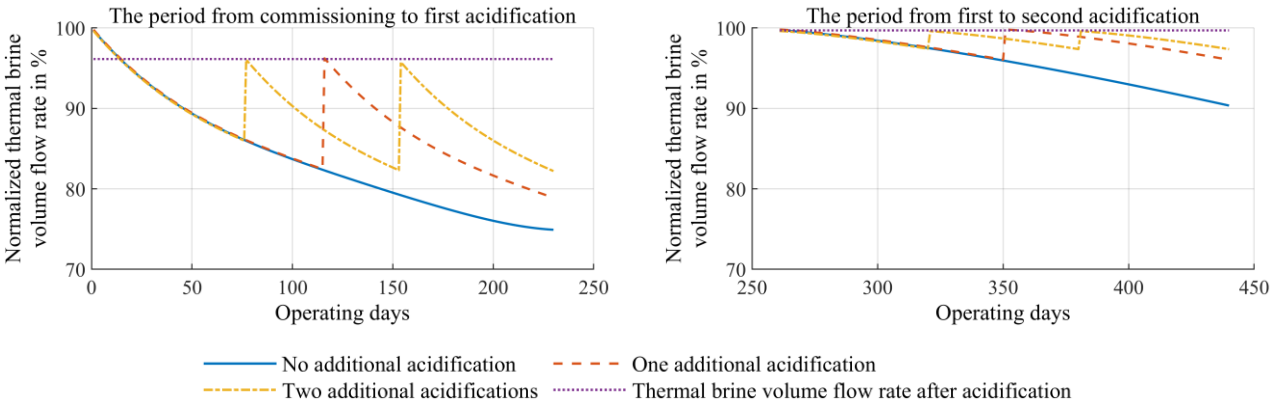

Figure 11: Assumed thermal brine volume flow rate for the three investigated scenarios with no, one and two additional acidifications of the ESP 1 in Geothermal Plant C in the two considered periods

4.2 Evaluation of the amount of electrical energy losses due to the deterioration of the thermal brine volume flow rate caused by scaling and its financial impact on geothermal power plants investigating different acidification intervals of the ESP 1 in Geothermal Plant C

With the approach described in the previous section applying the simulation model of the ORC power plant of Geothermal Plant C, the amounts of losses of produced electrical energy are calculated for the three investigated scenarios with no, one and two additional acidifications of ESP 1 in the two considered periods. Fig. 11 shows the cumulative financial losses due to reduced pump performance and costs for the three investigated acidification scenarios in the two considered periods, which are directly proportional to the amounts of losses of produced electrical energy due to the constant feed-in electricity tariff of 0.252 euro per kilowatt-hour guaranteed by the Renewable Energies Act in Germany. The cumulative financial losses for real operation without additional acidification amount to more than 700,000 euros. As shown in Fig. 11, the cumulative financial losses could be significantly reduced with one and two additional acidifications. Costs for the acidifications are not yet considered in the depicted curves for one as well as two further acidifications in Fig. 11, as the costs for one acidification may vary for different geothermal plants with regards to the installation depth of the ESP as well as disposal costs for reacted acid. However, the financial losses of produced electrical energy caused by the

production downtime of the ESP for its acidification are considered with a downtime period of 24 hours, although less time is needed for the acidification process. The reason for considering further downtime is the start-up and shutdown times of the ESP in which a lower thermal brine volume flow rate can be lifted. The difference in the cumulative financial losses in performing one and two additional acidifications amounts to 110,000 euros for the first period from commissioning to the first acidification of the ESP. The second period reveals different results. With regard to the much lower gradient of the reduction of the thermal brine volume flow rate of the second considered period compared to the first period, the cumulative financial losses are much lower for all investigated scenarios. Nevertheless, performing additional acidification within the second considered period would lead to a surplus profit, which is studied and evaluated in the following.

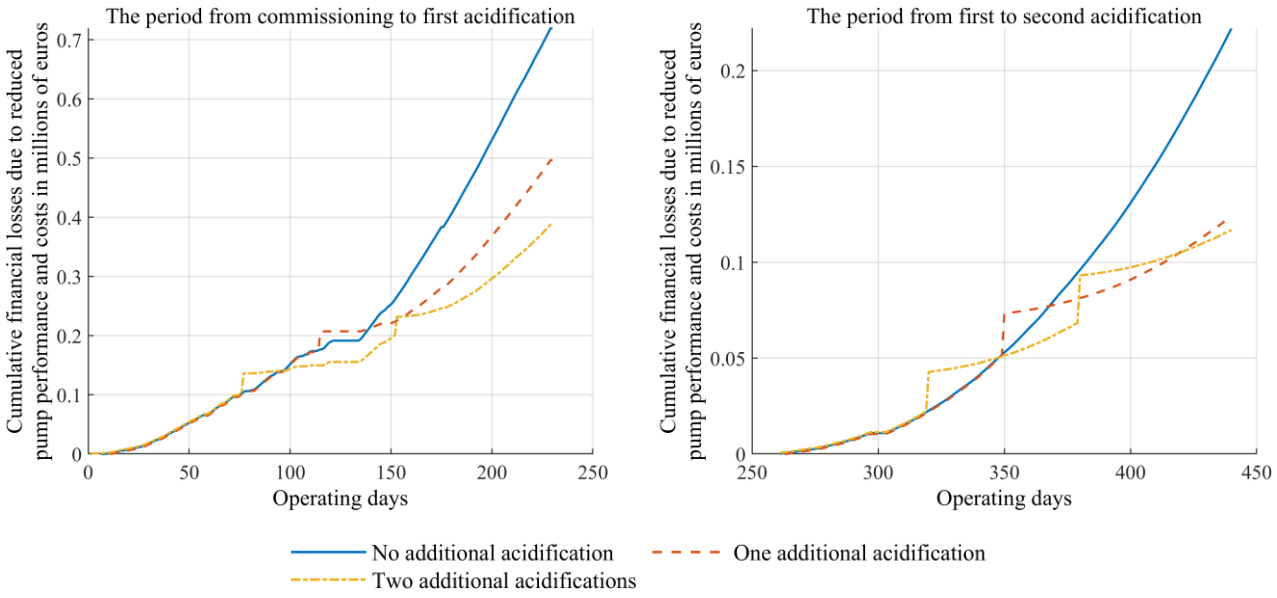

Figure 12: Cumulative financial losses due to reduced pump performance and costs for the three investigated acidification scenarios in the two considered periods

Figure 12 reveals the surplus profit dependent on the costs for one acidification of the ESP 1 in Geothermal Plant C for the investigated shorter acidification intervals with one and two further acidifications in the two considered periods. The cross of the lines for one and two additional acidifications in Fig. 12 marks the costs for one acidification of the ESP above which in the x-axis direction one additional acidification of the ESP is more rewarding than two additional acidifications. That means that if the costs for one acidification of the ESP in the first considered period were below 115,000 euros, the scenario with two additional acidifications of the ESP would have been more profitable. The surplus profits for the second considered period are much lower in comparison to the first period. Thus, it is unlikely that two acidifications would result in a higher surplus profit. Nevertheless, additional acidification of the ESP in the second period under consideration would have been worthwhile.

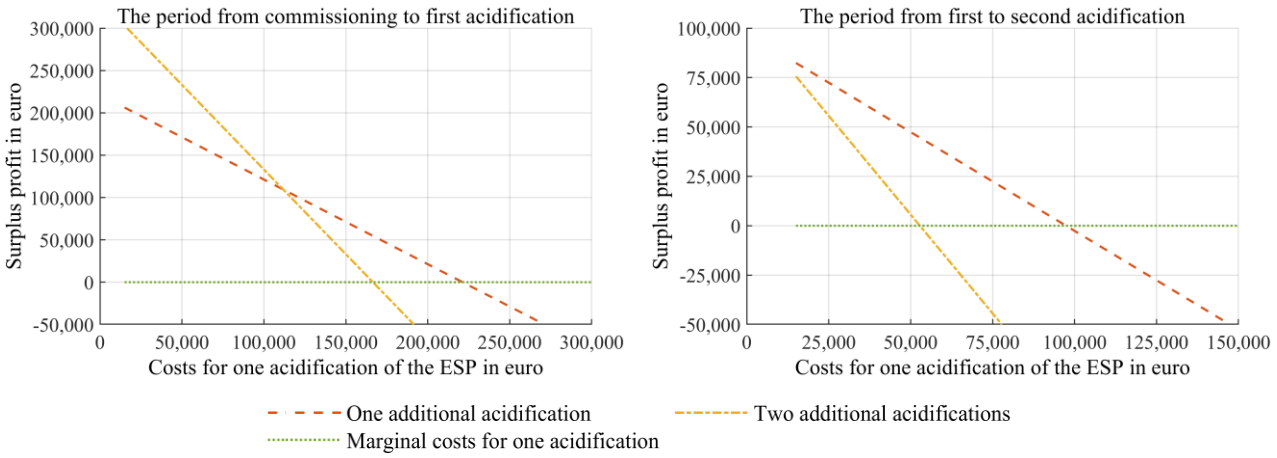

Figure 13: Surplus profit dependent on the costs for one acidification of the ESP 1 in Geothermal Plant C for the investigated shorter acidification intervals with one and two further acidifications in the two considered periods

5. CONCLUSION

The analysis of the long-term operational data of four considered electrical submersible pumps of three geothermal plants shows similar trends in the main operational metrics and key performance indicators concerning the impact of scaling. While degradation of the thermal brine volume flow rate is observed with increasing operating time at comparable AC power frequency for all

investigated ESPs, the mass-specific pump power is increasing over time. Acidifications of the ESPs improve the thermal brine volume flow rate significantly and reduce electrical power consumption. The overall delivery head of the investigated ESPs shows different behavior. For some ESPs the overall delivery head is for most of the operating time constant, for an ESP it reduces with the deterioration of the thermal brine volume flow rate, for another ESP it increases, which could be caused by changes occurring in the thermal water reservoir. The overall delivery head can also be increased by applying acidifications of the ESPs, as the detailed analysis of the first and second acidification of the ESPs shows. The ESP system efficiency is identified to detect and quantify the ongoing degradation process of ESPs due to scaling. It decreases from commissioning to first acidification or between acidifications and can be significantly enhanced by acidifications of an ESP. Scenario analysis with varying acidification intervals reveals that acidifications of the ESP performed every three months in the first operating year leads to a high surplus profit in contrast to the currently applied maintenance strategy with acidifications after more than a half year of operation of an ESPs. The gradients of the thermal brine volume flow rate and the ESP system efficiency shall be monitored to determine acidification times. With advanced lifecycle time of an ESP, the acidification intervals increase for optimized profitability.

ACKNOWLEDGMENT

Funding from the Bavarian State Ministry of Education, Science and the Arts in the framework of the project Geothermal-Alliance Bavaria is gratefully acknowledged. Furthermore, we would also like to show our gratitude to the Munich City Utilities (Stadtwerke München - SWM), which have provided significant support for our research by providing long-term operating data of their geothermal plants as well as useful knowledge and information.

NOMENCLATURE

Letter symbols

C	costs, EUR
DH	delivery head, m
f	frequency, Hz
g	gravitational acceleration, m/s²
I	revenues, EUR
$\dot{m}$	mass flow rate, kg/s
MSP	mass-specific pump power, W/(kg/s)
n	number of acidifications
P	power, W
$\dot{V}$	volume flow rate, m³/s

Subscripts and superscripts

acid	acidification
add	additional
down	downtime
el	electrical
fric	friction
geo	geodetic
sys	system
wh	wellhead

Greek symbols

ρ	density, kg/m³
η	efficiency

REFERENCES

Beebe, R.S.: Predictive maintenance of pumps using condition monitoring, Elsevier Science (2004)

DiPippo, R., Moya, P., Las Pailas geothermal binary power plant, Rincón de la Vieja, Costa Rica: Performance assessment of plant and alternatives, Geothermics 48, (2013), 1–15.

Eyerer, S., Schifflechner, C., Hofbauer, S., Wieland, C., Zosseder, K., Bauer, W., Baumann, T., Heberle, F., Hackl, C., Irl, M., others: Potential der hydrothermalen Geothermie zur Stromerzeugung in Deutschland. Technical University of Munich, Chair for Energy Systems, URL: https://mediatum.ub.tum.de/1360572, (2017)

Flechtner, F., Aubele, K.: A brief stock take of the deep geothermal projects in Bavaria, Germany 2018, *Proceedings*, 44th Workshop on Geothermal Reservoir Engineering, Stanford University, Stanford, California, February 11-13 (2019)

Frick, S., Regenspurg, S., Kranz, S., Milsch, H., Saadat, A., Francke, H., Brandt, W., Huenges, E.: Geochemical and process engineering challenges for geothermal power generation, Chemie Ingenieur Technik 83, (2011), 2093–2104.

Köhl, B., Baumann, T.: Scalings at geothermal facilities-Characterisation, processes and mass balance, EGU General Assembly Conference Abstracts, (2018), p. 13260.

Kullick, J., Hackl, C. Dynamic modeling and simulation of deep geothermal electric submersible pumping systems; *Energies 10*, (2017), p. 1659.

Milanovic, P., Jacimovic, B., Genic, S.: Experimental measurement of fouling resistance in the heat exchanger of a geothermal heating system. *Geothermics* 35, (2006), 79–86.

Ravier, G., Graff, J.-J., Villadangos, G.: Operating a lineshaft production pump in a small pump chamber under highly aggressive geothermal fluid conditions: Results from the Soultz EGS site, *Proceedings*, World Geothermal Congress, Melbourne, (2015)

Schifflechner, C., Eyerer, S., Alonso Alvarez, P., Wieland, C., Spliethoff, H.: Evaluating the South German Molasse Basin's geothermal potential by means of the UNFC 2009 Classification, European Geothermal Congress, (2019)

Wisotzky, F., Cremer, N., Lenk, S.: Angewandte Grundwasserchemie, Hydrogeologie und hydrogeochemische Modellierung. Berlin, Springer Spektrum, (2018), 83-120.

Zarrouk, S.J., Woodhurst, B.C., Morris, C.: Silica scaling in geothermal heat exchangers and its impact on pressure drop and performance: Wairakei binary plant, New Zealand. *Geothermics 51*, (2014), 445–459.